PII: S0032-3861(96)00812-9

Polymer Vol. 38 No. 11, pp. 2683–2688, 1997

0032-3861/97/$17.00 + 0.00

Orientation and conductivity in polyaniline: 1

C. D. G. Minto and A. S. Vaughan*
J.J. Thomson Physical Laboratory, University of Reading, Whiteknights, Reading RG6 6AF, UK
(Received 22 April 1996; revised 27 June 1996)

Films of polyaniline doped with (±)-camphor sulfonic acid, cast from *m*-cresol, exhibit considerable metallic properties. Such films are partially crystalline, but appear macroscopically disordered when probed by X-rays. Changing the X-ray geometry to probe molecular trajectories within the thickness of such films reveals considerable anisotropy; the molecules statistically adopt a chain direction parallel to the film surface. Some degree of ordering is also noted perpendicular to this, i.e. in the direction of the film thickness, indicating some alignment of the polymer/counter ion complex. We believe that the origin of this orientation lies in a complex interaction between molecule, dopant and solvent whereby the polymer adopts an extended, swollen conformation in solution. On removal of solvent these structures deposit as 'stiff logs'. Such orientation increases the intrinsic ordering within the materials, thus allowing metallic properties to be revealed. By selecting only one enantiomer for doping, less steric disruption is found and a more ordered structure with greater orientation can develop. Such materials exhibit a greater conductivity and enhanced metallic features as compared to polymers doped by (±)-camphor sulfonic acid. © 1997 Elsevier Science Ltd.

(Keywords: polyaniline; orientation; conductivity)

INTRODUCTION

Theoretical predictions for conducting polyaniline (PANI) have established that the Fermi level lies half way through a band[1], thus we expect the system to exhibit metallic properties, such as a finite conductivity at $T = 0$ K and a positive temperature coefficient of resistivity (PTCR). Experimental observations on PANI produced in the standard fashion (cast from NMP and protonated with HCl) all reveal transport characteristics indicative of insulating, disordered semi-conductors[2,3]. The origin of this discrepancy lies in disorder. It is well known that disorder induces electron localization[4] and if the magnitude of this disorder potential is comparable to the band-width, then complete localization will take place and the system will be an insulator. Weaker disorder introduces a mobility edge, separating localized electron states near the band tails from extended states further into the band. In this case, the position of the Fermi level (E_F) relative to the mobility edge (E_C) will determine whether the material will have insulating or metallic characteristics[5,6]. In the case of PANI–HCl, the above mentioned metallic signatures have not been observed; the behaviour of the resultant insulator has been explained by a number of theories, but most commonly as a phase separated mixture of metallic crystalline islands (delocalized electrons) embedded in an insulating amorphous sea (localized electrons)[3,7]. This combination of various scales of disorder is sufficient to render the material insulating.

Recent developments with camphor sulfonic acid/*m*-cresol systems have revealed some of the much hoped for metallic characteristics; a PTCR[8], a massive negative dielectric constant[9] and a linear thermoelectric power[10], amongst others, are all signatures of extended electron states. Whilst this is very encouraging, these advances have yet to be maximized; for example, the material properties could be improved through orientation, to a predicted[8] 1000–2000 S cm^{-1}. Molecular orientation in conducting polymers clearly is a desirable characteristic, improving both inter and intra chain transport.

However, without *any* orientation, the materials have, nevertheless, been classified as disordered metals close to the critical regime[8]. The existence of this metallic state has been attributed to improved structural order and fewer defects of the molecular scale[8], even though all reported studies have shown the material to be very similar to traditional PANI in that it is only ~ 50% crystalline with similarly small domain sizes.

The following results reveal that considerable intrinsic orientation does exist in solution cast films and that it is this decrease in structural disorder which allows the material's intrinsic metallic state to be partially revealed. An understanding of the origin of this structure can be gained by considering the observed behaviour together with a careful analysis of the existing literature. To our knowledge such an analysis, and the associated improvements in properties, have as yet been unreported. With these results being based on unoptimized films and further orientation opportunities still unexplored, the full possibilities of PANI (as a highly conductive, truly metallic, environmentally stable conductor) have yet to be realized.

EXPERIMENTAL

Emeraldine Base (EB) was synthesized at 0 ± 0.05°C in

---

* To whom correspondence should be addressed

the conventional manner[11]. The material was compounded with the stochiometric amount of (±)-CSA (Aldrich) (2:1 molar ratio of PhN group to CSA molecule) and dissolved in *m*-cresol for 24 h. The resultant dark green solution was centrifuged or vacuum filtered to remove a minor insoluble part. The films were cast, covered for 24 h, and then dried on a hotplate at 40–50°C. The resulting high quality films are easily removed and appear to be black by reflected light and green by transmission. For films produced using a selected enantiomer, (+)-camphor sulfonic acid (CSA) (Aldrich), the procedure used was identical. X-ray measurements were recorded using flat plate film on a Philips PW1120/90 generator running at 40 kV/40 mA producing a monochromatized, nickel filtered CuK_α ($\lambda = 1.541$ Å) beam. Similarly, a computer controlled diffractometer was used to scan in q ($= 2\pi/d$) from $q = 0.2$ Å^{-1} to $q = 4.0$ Å^{-1} in steps of $\delta q = 0.02$ Å^{-1}. Rotation in the plane perpendicular to the beam was performed from $\alpha = 0°$ to $360°$ in steps of $\delta\alpha = 6°$. The sample geometry for such experiments has been discussed by Mitchell *et al.*[12]. To probe the specimen orientation in the plane of the film ($\chi = 0°$), films were mounted in the conventional manner. For $\chi = 90°$ experiments, small strips were sectioned from the film and mounted with the film surface parallel to the X-ray beam and oriented vertically; in this configuration the X-ray beam penetrates the film thickness. All sample to film distances were calibrated using silicon powder which exhibits a characteristic Bragg angle of $2\theta = 28.46°$.

Conductivity data were gathered using the four probe technique on free standing films to evaluate the resistance, contacts were made using copper wire and conducting carbon cement, the film resistance was measured from liquid nitrogen (~ 80 K) to room temperature (~ 290 K).

RESULTS

A typical diffractometer trace for a PANI-CSA(±) film in the standard ($\chi = 0°$) configuration is shown in *Figure 1*. This trace is uncorrected for diffuse background or amorphous scattering. As can be seen, the trace consists of a number of reasonably well defined peaks, together with some less intense information. Most peaks are easily resolved on a flat plate and can be seen to exhibit no arcing. Although almost hidden by amorphous scattering, the peaks at 5.2 and 4.6 Å are sharp and can clearly be discerned on a flat plate. All derived X-ray scattering information from this and other samples is tabulated in *Table 1*.

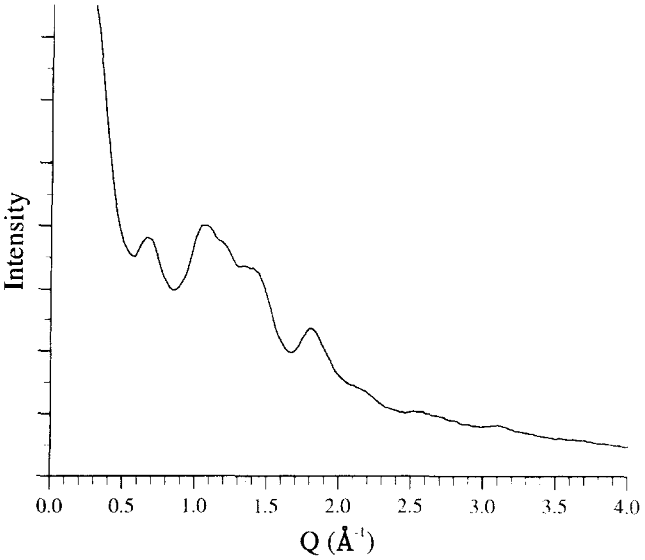

Figure 1 Diffractometer trace for (±)-CSA doped films in the $\chi = 0$ configuration

The appearance changes quite dramatically when viewed in cross-section ($\chi = 90°$); a typical flat plate exposure together with a schematic representation of the observed reflections are shown in *Figure 2* and diffractometer traces for equatorial and meridional scans for the above configuration are shown in *Figure 3*. As can be seen, considerable anisotropy is present. In the diffractometer trace this is most evident in the 9.2 and 3.5 Å peaks.

To summarize briefly, for a sample oriented with the surface plane of the film lying vertical, peaks at 20, 4.4, 3.5 and 2.9 Å exhibit arcing (or areas of increased intensity) along the equatorial direction; peaks at 9.2, 5.2, 4.6, 2.4 and 2.0 Å show arcing along the meridian. The peak at 6.0 Å shows strong off axis orientation centred on 45°, 135°, etc.

An estimate of the degree of ordering can be obtained by recording peak intensities[13] as the sample is rotated around the beam axis (α), i.e. the intensity of the circumference of a circle of fixed radius on a flat plate. The order parameter ($\langle P_2 \rangle$) is subsequently extracted by fitting the intensity variation (compared to background) to a series of even order Legendre polynomials. A fully oriented system will give an order parameter of 1 and an unoriented system will similarly give 0.

Utilizing this operation, we find order parameters of 0.39 for the 3.5 Å (equatorial) peak and 0.33 for the 9.2 Å (meridional) peak. This reveals that the material is highly anisotropic; such orientation parameters are very high for a material which has not been subjected to an external influence such as deformation or poling.

Figure 4 shows equatorial and meridional traces collected from a sample of polymer produced using (+)-CSA (in the $\chi = 90°$ configuration). As can be seen, the crystalline peaks are similarly placed to those in the previous figure (these are again listed in *Table 1*) and again, the same intrinsic molecular ordering is found on rotation of the specimen. For the samples analysed here, we see an increase in the orientation parameter derived from the 3.5 Å peak from 0.39 to a quite astounding 0.50. In the meridional 9.2 Å peak, no significant increase is noted, the parameter staying around 0.32. These changes

Table 1 *d* spacings for PANI–CSA films, orientation and relative intensity

(±)-CSA				(+)-CSA			
Q(Å^{-1})	d(Å)	Orient.	Strn	Q(Å^{-1})	d(Å)	Orient.	Strn
~ 0.3	~ 20	⊥	m	~ 0.3	~ 20		s
0.68	9.2	‖	s	0.68	9.2	‖	m
1.05	6.0	45	s	1.06	5.9	45	s
1.20	5.2	‖	s	1.23	5.2	‖	m
1.36	4.6	‖	s	1.42	4.4	‖	m
1.42	4.4	⊥	m	1.8	3.5	⊥	w
1.78	3.5	⊥	vs	2.1	2.9	⊥	vs
2.2	2.9	⊥	w	2.7	2.3		vw
2.6	2.4	‖	vw				
3.1	2.0	‖	vw				

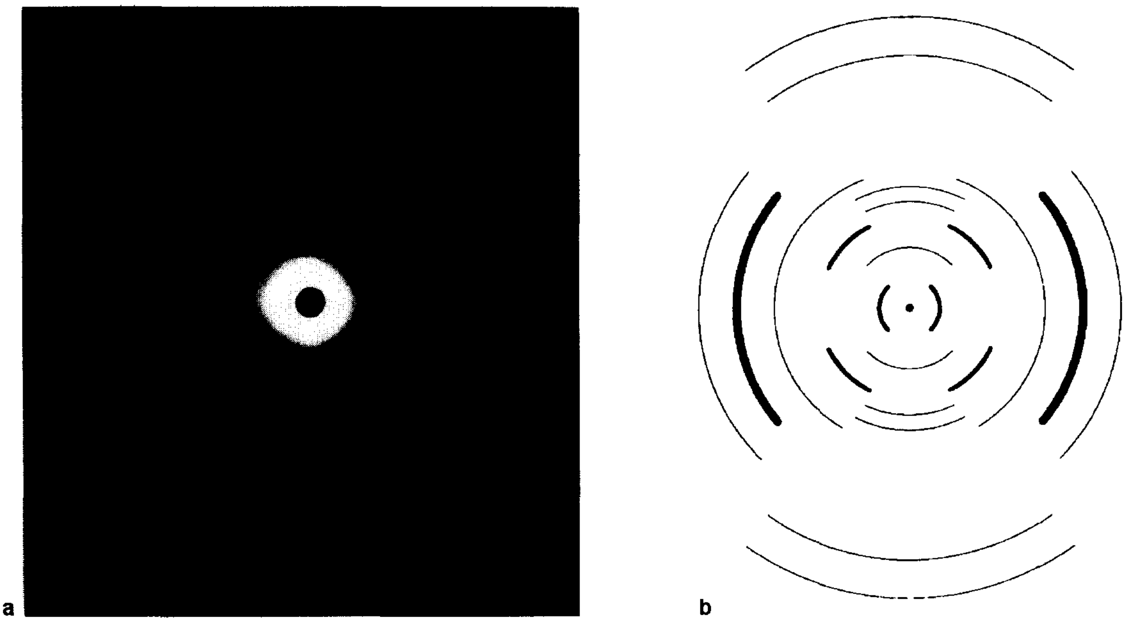

Figure 2 (a) Flat plate of PANI (±)-CSA in the $\chi = 90°$ configuration; (b) schematic representation

are easily reproducible. Noticeably, the scattering intensity of the peaks is considerably lower than that found in films produced using (±)-CSA, however all reflections are still present, this will be discussed later.

PANI films cast from *m*-cresol are known to exhibit charge transport behaviour suggestive of a system at the critical region of the metal/insulator transition. *Figure 5* compares the conductivity of (±)-CSA and (+)-CSA films over a limited temperature range; *Figure 5a* shows the data using (±)-CSA as the counter ion and *Figure 5b*, the conductivity for a film produced using only (+)-CSA.

Consider first the racemic mix. The trace has three important features, a negative temperature coefficient of conductivity above ~ 250 K, a positive coefficient below this and a complete range not spanning a decade i.e. effectively flat as compared to traditional PANI-HCl films. This behaviour has previously been explained[8] in terms of Larkin–Khmel'nitskiĭ power law behaviour in the critical regime[14] (where E_C is close to E_F) or as a phonon mediated quasi-1D model resulting as a superposition of band and phonon-assisted transport[15]. The absolute magnitude of the conductivity results presented here are slightly lower than those generally reported, perhaps due to non-optimal deposition conditions, but the overall trends are in line with previously published results.

For films produced using the isolated enantiomer, significantly, the room temperature conductivity is greater than that of the (±)-CSA films produced using identical procedures, giving a value of ~ 280–300 S cm^{-1}. Again very little variation of conductivity with temperature is observed, between 77 K and room temperature only a variation of 20 S cm^{-1} is seen. Notably, the position of the maximum in the curve has moved downwards to below 200 K; clearly the films are more metallic. As yet we have not been able to probe down to liquid helium temperatures and thus analyse the

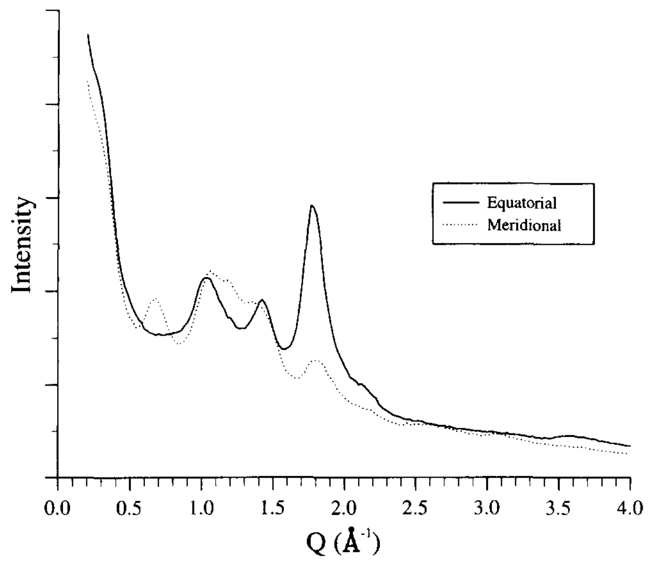

Figure 3 Meridional and equatorial scans for (±)-CSA doped films in the $\chi = 90°$ configurations

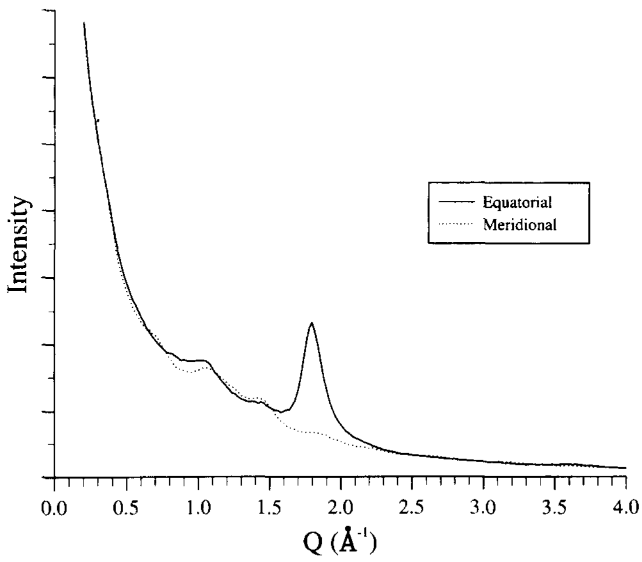

Figure 4 Diffractometer traces for (+)-CSA doped films in the $\chi = 90°$ configurations

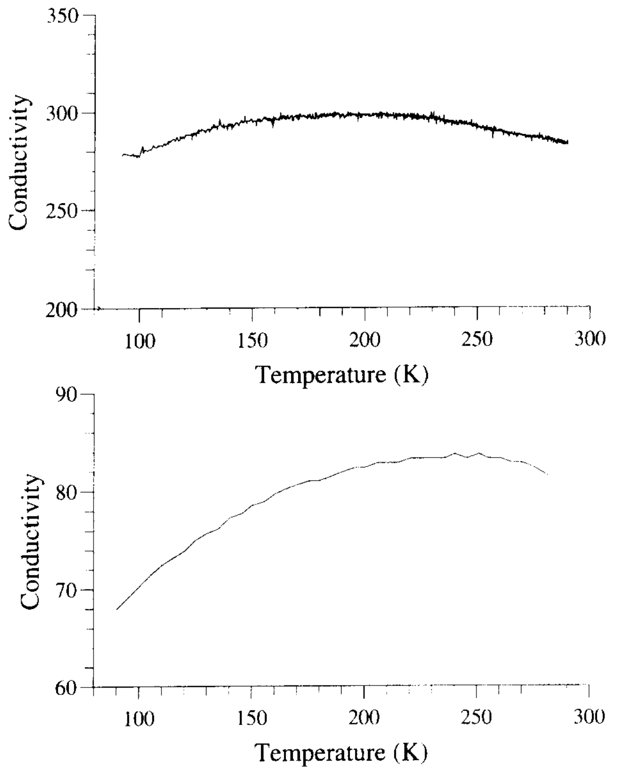

Figure 5 Conductivity of polyaniline films cast from *m*-cresol using (±)-CSA (bottom: a) and (+)-CSA (top: b)

reduced activation energy and so placement of the materials on the metal insulator spectrum is rather difficult. However, the traces exhibited from our (±)-CSA are similar to those previously published in the literature, films which have been shown to pass over into extended electron states, the mobility edge being lower than the Fermi level. With this in mind, these films of (+)-CSA clearly represent a considerable improvement.

DISCUSSION

Anisotropy is clearly evident in our specimens but, in order to interpret the results fully, the anisotropy must be correlated to the main chain direction. Although the crystallographic structure of PANI–HCl has been intensively investigated and modelled[16], very little is known about the structure of PANI–CSA. To our knowledge, only three remotely detailed expositions of the PANI–CSA structure have been published. Pouget *et al.* described the WAXS behaviour of films of PANI–CSA under various processing conditions[17]. This was followed by a study of PANI and POT–CSA (poly*ortho*-toluidine) fibres[18]. Similarly, Cao *et al.* discussed briefly the behaviour of PANI–CSA fibres[19]. In fibres, Pouget observed[18] oriented reflections in the [001] direction at 9.2 and 4.6 Å, with the 9.2 Å reflection being interpreted as d_{001}. Reflections at 20 and 3.5 Å were seen to orient themselves perpendicular to the chain direction; the 5.9 Å reflection exhibited no preferential orientation. These reported results agree very well with ours presented above, with the anisotropy lying in the corresponding inter- and intramolecular directions. Our results therefore indicate that the average trajectory of the molecular chains *within unextended films* lies preferentially parallel to the film surfaces. Supporting this is the fact that the 3.5 Å reflection is both the strongest and is oriented in the equatorial direction, indicating that a significant number of molecules are therefore stacked parallel to the plane of the film with an average separation of 3.5 Å (as was also concluded by Pouget *et al.* in the case of fibres). Similarly, there is significant orientation of the larger 20 Å reflection. Along the chain direction, we find the (001) reflection exhibiting strong orientation at 9.2 Å with other reflections following suit. If we interpret this as the length of the unit cell, then there is a reasonably strong correlation between the stacked layers of polymer. The resultant picture is similar to that found in electrochemical polymerization of pyrrole[20], although the deposition mechanism is clearly different.

An interchain separation of only 3.5 Å, is much smaller than that found in the ES-I and ES-II, structures where the separation is at 4.4 Å[16]. In the ES structures, there is a reasonable dihedral angle associated with out of plane twisting of the phenyl rings. In order for this to be decreased to only 3.5 Å (very close to a separation of graphitic carbon rings) the molecules must adopt a planar conformation. The driving force behind this rotation will be discussed later. Of particular interest here is the 20 Å reflection. This is harder to correlate to any unit cell due to its magnitude; at 20 Å it is six times greater than the molecular separation and almost as large as the crystallographic coherence length!

Recently it has been suggested by Majidi *et al.*[21] that PANI doped preferentially with the selected + or −(*d*, *l*) enantiomorphs of CSA forms strongly chiral, helical screws in solution. Similarly, in an early study of PANI–(±)CSA solutions, Cao and Smith[22] discovered the presence of a liquid crystalline, lyotropic phase in sheared solutions. Using this racemic dopant, the rods in solution were characterized as having a width of 20 Å. The origin of these two phenomena are presumably related. Similarly, Cao *et al.* directly correlated their X-ray scattering results[19], quoted above, to the chiral behaviour observed in solution, the results being interpreted as scattering from helical screws with 2_1 symmetry. The authors suggested that the PANI conformation in the solid would be similar to that found solution.

In the data presented here, an equatorially oriented reflection of 20 Å is observed and we feel that this must strongly be related to the 20 Å width of the rods found in lyotropic solutions by Cao *et al.* Stiff rods will preferentially be deposited lengthwise to give an oriented structure such as that described above, they would however not sediment with any particular directional ordering with respect to the plane of the film, again, as is observed above.

The origin of this rod like behaviour (which has not been quoted as occurring in chloroform deposited films) lies in the nature of the interaction between polymer, counter ion and solvent. In a recent paper, Ikkala *et al.*[23] investigated, theoretically, molecular recognition effects in PANI. The authors found a strong association between the carbonyl group in CSA and hydrogen bonding donors such as the hydroxyl group in *m*-cresol and concluded that the resulting hydrogen bond can manipulate the orientation of the solvent molecules. An optimized molecular structure which includes such interactions, is one where the phenyl rings of the solvent and the molecule interact via van der Waals forces, to adopt a co-planar configuration, with a separation of 4.8 Å (when there is no pressure from stacking from other molecules). The authors suggested that the complex would form such a stacked structure in the amorphous regions; in the crystalline regions no *m*-cresol would remain, but the planar conformation of the molecules would nevertheless be retained (but presumably at a smaller inter-molecular separation). In accordance with this, it has been noted[17] that there is a significant increase in the percentage of crystalline material within the films as they are aged, i.e. concomitant with the loss of *m*-cresol.

One can estimate, therefore, that if the molecular complex were to be stacked in a random (non-crystalline) manner then the separation would be of the order of 18–20 Å: $\{(\text{width of molecule}) + 2 \times (\text{separation of molecule and solvent}) + (\text{inter complex separation})\}$. This factor accounts for the large reflection in the intermolecular separation direction, this reflection purely being associated with non-crystalline regions which have not lost their *m*-cresol. Similarly the width of the molecule, assuming a degree of cylindrical symmetry for the partially extended polymer, will be of the order of 20 Å, thus accounting for the dimensions observed in the solution behaviour.

The X-ray scattering behaviour can, we propose, be accounted for by considering the reflections to arise from two distinct phases. In the crystalline phase, PANI exists in a planar configuration, the molecules lying parallel to the plane of the film. The planar configuration, brought on by the *m*-cresol, allows a reduction in the (100) reflection from $a = 4.26$ Å for ES-I (HCl protonated)[16] to $a = 3.5$ Å as observed here. The unit cell length along the c axis is similar at $c = 9.2$ Å. The (010) reflection is harder to identify since, if we assume that there is no preferential deposition direction, this reflection should have an orientation similar to that of the 9.2 Å reflection. The obvious candidate therefore is the reflection at 5.2 Å. This is significantly smaller than that observed in ES-I (5.94 Å), but as this distance is highly dependent on both the conformation of the molecule and counter ion, this is still possible. A large portion of the remaining disorder will be steric in nature, arising from the chiral nature of the counter ion—this will be discussed more later. The arced reflection at 6.0 Å, indexed as being oriented off axis, is interesting and is possibly due to a (021) reflection from well packed planes of phenyl rings (on the N–N direction). Finally, a schematic description of the behaviour of the molecules in both the crystalline and amorphous regions is shown in *Figure 6*.

Presumably if the large 20 Å reflection is entirely due to the presence of the *m*-cresol 'swelling' the molecule then, on complete removal of the remaining bound solvent (~ 16%), we would expect the inter-molecular separation of the molecules to approach more closely that of the crystalline regions noted above. Similarly, we would expect the degree of orientation to be increased as there will be less freedom for rotation of molecules. This is indeed what we observe. After heating the same (+)-CSA specimen under vacuum for 3 days at 100°C, the results shown in *Figure 7* were obtained. The 20 Å reflection has disappeared and we are left with very oriented reflections*. We find an increase in orientation of the 3.5 Å reflection from 0.5 to 0.6.

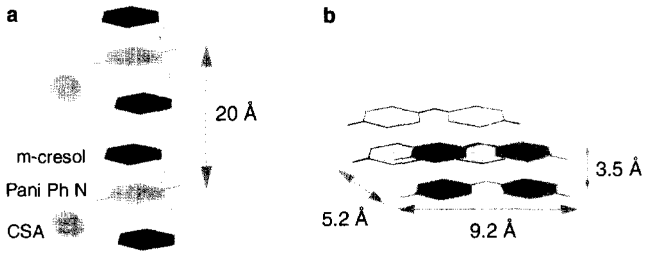

Figure 6 Schematic diagram suggesting the conformation of PANI in (a) amorphous regions and (b) crystalline regions

We are now in a position to ascribe the conductivity performance enhancements to structural factors. Transport in crystalline regions of PANI has been traditionally thought of as metallic, the insulating characteristics of the bulk brought about by degradation due to the granular structure of the material (metallic islands in an amorphous sea). In PANI–CSA, there are two definite enhancements that can be noted. The interchain separation within the crystalline fraction has been reduced, due to the planar stacked structure of the molecules (to 3.5 Å). This will result in more extended interchain transfer integrals, and hence an improved delocalization length (this we stress is solely for the metallic regions). More importantly for the macroscopic conductivity, the extended and oriented nature of the whole material, significantly decreases the amount of disorder within the insulating regions. Indeed, the organization within the amorphous regions closely reflects that in the crystalline regions.

We therefore have a picture of metallic crystallites, connected by molecular links; the amorphous sea. These molecular links, themselves being oriented and, as a consequence, less tangled, possess a more extended conformation. Since the type of transport within the bulk material is entirely mediated by the amount of disorder present within the amorphous regions, we here have a revealing explanation as to how extended transport within these new polyanilines is allowed. As discussed earlier, the disorder potential will be significantly reduced allowing the materials to approach a

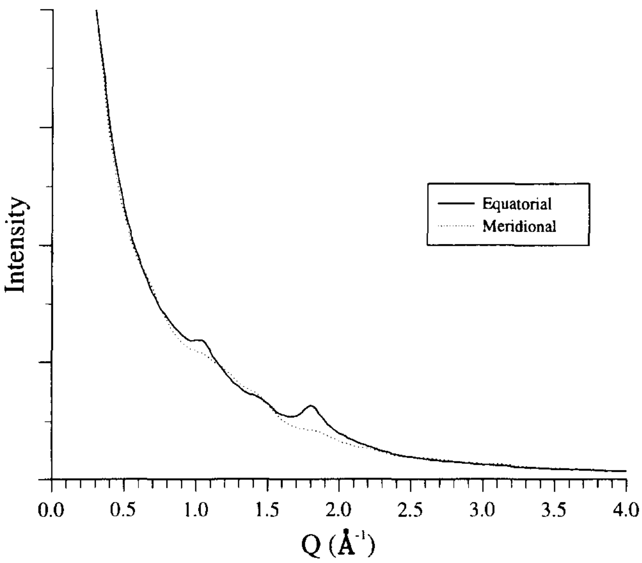

Figure 7 Diffractometer traces for (+)-CSA doped films which have been heated to extract *m*-cresol

---

*Although the orientation appears less in the diagram, the intensity values of the meridional scan at 3.5 Å are very close to the background count giving the high orientation values metallic state with extended wavefunctions. With no preferential ordering within the plane of the film, macroscopic transport will still be hindered somewhat, ensuring that E_F is still close to, but slightly greater than E_C.

In the standard materials discussed above, the dopant comes as a racemic compound; this will give rise to some steric disruption within both the insulating and crystalline regions. This effect will also be very pronounced in solution. Since we have competing left and right handed dopants, if the nature of the interaction is such that the polymer is forced into a preferential conformation, presumably competing left and right handed parts will tend to disorder the chain more than if only one species was present. On this basis we would expect by selecting either the dextro (+) or laevorotatory (−) form, a more sterically uniform main chain, greater anisotropy of deposition, much better packing and presumably conductivity benefits. As can be seen above, this is indeed the case. On replacing the dopant with only the dextro form, significantly better packing is observed, giving much greater alignment of the planes of PANI molecules. As expected, the conductivity results also show improvements. Most of the reflections such as the *c* axis unit length at 9.2 Å and the intermolecular separation (*a* axis) exhibit no major changes. The major improvement is hence not crystalline in nature but in the packing exhibited by the deposited 'logs'.

Finally, we observe a notable decrease in scattering intensity in films produced using (+)-CSA as the dopant. Whilst a more indepth scattering study is needed to explain this anomaly, it can be shown, by studying films of similar thickness, that this decrease is *not* due to any increase in absorption. This, therefore, only leaves the possibility that the films scatter less. Although most reflections are still visible, it is evident that the only strong scattering peak remaining is that due to the interchain packing (3.5 Å). As we have discussed above the increase in anisotropy is due to more uniform logs deposited from solution. It is, however, quite conceivable that racemic geometries may allow better crystalline packing—it is much easier to consider tiling a mix of left and right handed shapes than purely single handed. This viewpoint is not at odds with the increase in anisotropy observed, presumably the selected dopant allows improved rods in solution which deposit in a more ordered arrangement, *but*, the percentage crystallinity may be reduced due to the arguments noted above and hence we see less intense scattering peaks.

CONCLUSION

By observing the X-ray scattering behaviour within the plane of conducting PANI films, we find considerable anisotropy, with the polymers adopting a trajectory parallel to the plane of the film. Orientation parameters of up to 0.39 have been observed so far. We suggest that this orientation is achieved by the dopant and solvent forcing the molecule into a planar, more extended configuration. The better transport characteristics of PANI–CSA can then be ascribed to both the reduced interchain separation within the crystalline regions and more importantly, to the macroscopic ordering that results within both amorphous and crystalline regions. Removing the remaining bound solvent forces the material into a very highly ordered conformation. By utilizing only selected right handed counter ions, the steric nature of the molecules in solution is improved greatly and better packing on deposition follows. This results in large orientation parameters up to 0.5 (before complete solvent removal), indicating very good alignment. This improvement over conventional CSA processing routes, confers significant conductivity enhancements giving very highly metallic polyaniline. With orientation of the polymers within the plane of the film still unexplored, significant improvements to the quality of the materials and thus to the conductivity, are still to be achieved.

ACKNOWLEDGEMENTS

The authors wish to thank Professor G.R.Mitchell for helpful discussions on the scattering behaviour. One of us, C.D.G. Minto, is grateful to the EPSRC for the funding of a PhD studentship.

REFERENCES

1. Brédas, J. L. In *Conjugated Polymers and Related Materials*, eds. L. Lundström W.R. Salaneck and B. Rånby. Oxford University Press, Oxford, 1993, pp. 187–221.
2. Wang, Z. H., Ray, A., MacDiarmid, A. G. and Epstein, A. J., *Phys. Rev. B*, 1991, **43,** 4373.
3. Wang, Z. H., Scherr, E. M., MacDiarmid, A. G. and Epstein, A. J., *Phys. Rev. B*, 1992, **45,** 4190.
4. Anderson, P. W., *Phys. Rev.*, 1958, **109,** 1492.
5. Mott, N. F. and Davis, E. A., *Electronic Processes in Non-crystalline Materials*, 2nd Edn. Clarendon Press, Oxford, 1979.
6. Mott, N., *Conduction in Non-crystalline Materials*. Clarendon Press, Oxford, 1993.
7. Li, Q., Cruz, L. and Phillips, P., *Phys. Rev. B*, 1993, **47,** 1840.
8. Reghu, M., Cao, Y., Moses, D. and Heeger, A. J., *Phys. Rev. B*, 1993, **47,** 1758.
9. Joo, J., Oblakowski, Z., Du, G., Pouget, J. P., Oh, E. J., Weisinger, J. M., Min, Y., MacDiarmid, A. G. and Epstein, A. J., *Phys. Rev. B*, 1994, **49,** 2977.
10. Yoon, C. O., Reghu, M., Moses, D., Heeger, A. J. and Cao, Y., *Phys. Rev. B*, 1993, **48,** 14080.
11. Wei, Y., Jang, G. W., Hsueh, K. F., Scherr, E. M., MacDiarmid, A. G. and Epstein, A. J., *Polymer*, 1992, **33,** 314.
12. Mitchell, G. R., *Polymer*, 1986, **27,** 346.
13. Mitchell, G. R. and Windle, A. H., *Polymer*, 1983, **24,** 1513.
14. Larkin, A. I. and Khmel'nitskiĭ, D. E., *Sov. Phys. JETP*, 1982, **56,** 647.
15. Joo, J., Prigodin, V. N., Min, Y. G., MacDiarmid, A. G. and Epstein, A. J., *Phys. Rev. B*, 1994, **50,** 12226.
16. Pouget, J. P., Józefowicz, M. E., Epstein, A. J., Tang, X. and MacDiarmid, A. G., *Macromolecules*, 1991, **24,** 779.
17. Pouget, J. P., Oblakowski, Z., Nogami, Y., Albouy, P. A., Laridjani, M., Oh, E. J., Min, Y., MacDiarmid, A. G., Tsukamoto, J., Ishiguro, T. and Epstein, A. J., *Synth. Met.*, 1994, **65,** 131.
18. Pouget, J. P., Hsu, C. H., MacDiarmid, A. G. and Epstein, E. J., *Synth. Met.*, 1995, **69,** 119.
19. Cao, Y. and Smith, P., *Synth. Met.*, 1995, **69,** 191.
20. Minto, C. D. G. and Vaughan, A. S., *J. Mater. Sci.*, 1995, **30,** 6028.
21. Majidi, M. R., Kane-Maguire, A. P. and Wallace, G. G., *Polymer*, 1995, **36,** 3597.
22. Cao, Y. and Smith, P., *Polymer*, 1993, **34,** 3139.
23. Ikkala, O. T., Pietilä, L., Ahjopalo, L., Österholm, H. and Passiniemi, P. J., *J. Chem. Phys.*, 1995, **103,** 9855.